Ocean Dynamics (2021) 71:157–173
https://doi.org/10.1007/s10236-020-01438-5

# Seasonal variations in the water residence time in the Bohai Sea using 3D hydrodynamic model study and the adjoint method

Chongxin Luo[1] · Lei Lin[2] · Jie Shi[1] · Zhe Liu[1,3] · Zhongya Cai[4] · Xinyu Guo[1,5] · Huiwang Gao[1]

Received: 27 August 2020 / Accepted: 26 December 2020 / Published online: 5 January 2021


**Abstract**

The Bohai Sea is a large, semi-enclosed bay of China with a transport timescale of more than 1 year. Residence time (RT) is an important indicator used to determine the water exchange rate of coastal oceans, and it has a significant influence on coastal ecosystems and the environment. In this study, the RT and its seasonal variability within the Bohai Sea were investigated using a 3-D hydrodynamic model and the adjoint method of the RT. The model results show that the annual mean RT in the Bohai Sea is 3.43 years, and the RT increases from the Bohai Strait to the northwestern coast. The seasonal variability of the RT averaged over the entire Bohai Sea is not obvious; however, the regional RT has a significant seasonal variation, which could be more than 290% on average. When the monsoon winds were removed from the model, the sensitivity experiment showed an annual mean RT increase of ~90% with negligible seasonal variations in most areas of the Bohai Sea. The wind-induced residual current controls the seasonal variation in ocean circulation and induces the seasonal variability in RT; thus, monsoon winds play a dominant role in the seasonal variations of the water exchange rate in the Bohai Sea. Sensitivity experiments also suggest that tides can slow the water exchange rate, whereas the baroclinic processes and river runoff can accelerate the water exchange rate in the region near the Yellow River estuary. This study highlights the critical role of monsoon winds in affecting seasonal variabilities in the coastal transport timescale and exchange rate.

**Keywords** Residence time · Seasonal variation · Monsoon winds · Adjoint method · Bohai Sea

## 1 Introduction

The transport of water and its exchange rate in coastal areas are important factors affecting the spatial and temporal distribution of marine organisms, nutrients, and pollutants (Bolin and Rodhe 1973; Takeoka 1984; Delhez et al. 2014). They also have important impacts on marine primary productivity, and the carbon and nitrogen cycles (Santos et al. 2009; Liu et al. 2019). As the self-purification of coastal oceans mainly depends on the exchange of water with the open ocean, the coastal water exchange rate has drawn wide attention from oceanographers (Liu et al. 2004; Wan et al. 2013; Du et al. 2018; Lin and Liu 2019a; Liu et al. 2019).

Residence time (RT) is an important indicator for quantifying the transport timescale and water exchange rate, which is defined as the time that a water parcel needs to leave the control region. The RT of seawater within a region considers the complete movement of a water parcel and it can reflect spatiotemporal differences in the water exchange within the region (Bolin and Rodhe 1973; Zimmerman 1976; Takeoka 1984). With the development of the constituent-oriented age and residence time theory (CART: Deleersnijder et al. 2001; Delhez and Deleersnijder 2002; Delhez et al. 2004, www.climate.be/CART), RT is widely used as an indicator in research on coastal hydrodynamics and the associated environment, such as the transport of pollutants and nutrients into the open ocean (Liu et al. 2004; Shen and Haas 2004; Gong et al. 2008).

Responsible Editor: Guoping Gao

✉ Zhe Liu
zliu@ouc.edu.cn

[1] Key Laboratory of Marine Environment and Ecology (Ministry of Education), Ocean University of China, 238 Songling Road, Qingdao 266100, China

[2] College of Ocean Science and Engineering, Shandong University of Science and Technology, Qingdao 266590, China

[3] Present address: Department of Earth Sciences, National Natural Science Foundation of China, Beijing, China

[4] State Key Laboratory of Internet of Things for Smart City and Department of Civil and Environmental Engineering, University of Macau, Macau, China

[5] Center for Marine Environmental Studies, Ehime University, 2-5 Bunkyo-Cho, Matsuyama 790-8577, Japan

Owing to the complexity and variability of hydrodynamics in the coastal ocean, RT often shows strong spatiotemporal variations with respect to multiple dynamic factors (Gourgue et al. 2007; Li et al. 2009; Cheng et al. 2019; Lin and Liu 2019a). Du and Shen (2016) found significant interannual and seasonal variations in RT within the Chesapeake Bay, which was mainly related to river runoff, and Sun et al. (2014) found that there were large differences in the RT within an estuary between dry and wet seasons. River runoff is one of the most important factors influencing coastal RT, especially in estuarine areas, whereas tidal effects play a more important role in the water exchange within shelf seas (because the effect of river runoff is weaker) (Yuan et al. 2007; Lin et al. 2015; Lin et al. 2020). Wind is also an important factor affecting the coastal RT. For example, Safak et al. (2015) found that wind decreased the RT of water in the Virginia Coast Reserve, and the effect of wind on the RT was more significant in relatively confined bays. In addition, Zhang et al. (2019) found that local wind reduced the RT in Daya Bay by intensifying the upwelling (downwelling) circulation, and it had substantial effects on the spatial distribution of RT therein.

The Bohai Sea, including the Liaodong Bay (LDB), Bohai Bay (BHB), Laizhou Bay (LZB), Central Basin (CB), and Bohai Strait (BS), is a semi-enclosed bay with an area of 77,000 km$^2$, and an average depth of 18 m. The BS is the only channel of exchange between the Bohai Sea and the external waters (Fig. 1) (Wang et al. 2008; Liu et al. 2012). Water flows into the Bohai Sea through the north and out through the south of the BS at a transport rate of 0.14 Sv in winter and 0.2 Sv in summer (Duan et al. 2020; Wu et al. 2019). The Bohai Sea is affected by a typical monsoon climate, and the hydrodynamic environment of the sea is complex with significant seasonal variation. The statistical results from monthly averaged European Remote Sensing Satellites (ERS-1/2) wind stress measurements (http://www.ifremer.fr/cersat) showed that the prevailing wind direction is NW in the autumn and winter, and S-SE during the remaining seasons (Wang et al. 2008). In addition, many seasonal rivers flow into the Bohai Sea, with a total annual average river runoff of $> 5.0 \times 10^{10}$ m$^3$, of which the Yellow River contributes > 50% of the total volume (Bulletin of Chinese River sediment 2015; Ding et al. 2020). The seasonal variability of the circulation within the Bohai Sea is well documented (Duan et al. 2020; Guo et al. 2018; Wang et al. 2008; Wei et al. 2001; Wu et al. 2019; Zhou et al. 2017). In the autumn and winter, the residual current is towards the south and southeast in the central CB, counterclockwise in the southern part of the BHB and LZB, and clockwise in the LDB (Guo et al. 2018; Wang et al. 2008). In the spring and summer, the residual currents in the three bays are counterclockwise, the water in the central CB moves north, and there are small residual vortexes in the Bohai Sea (Wang et al. 2008; Wei et al. 2001; Zhou et al. 2017). The

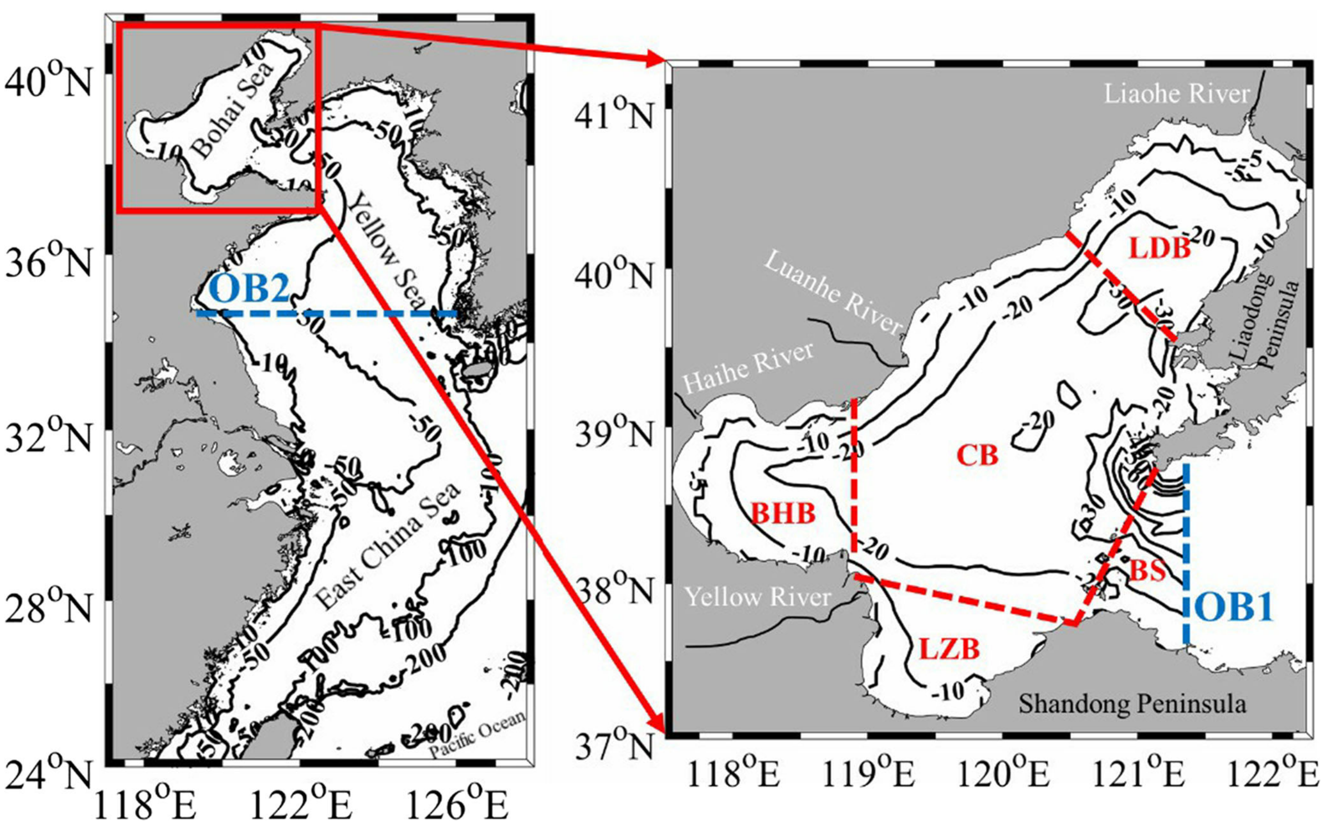


**Fig. 1** Water depth (m) and subdomains within the Bohai Sea. OB1 and OB2 are the boundaries of the control region and the computational region of the RT model, respectively

residual current in the BS in winter is similar to that in summer, except the residual vortex in the central BS (Guo et al. 2018; Wei et al. 2001;).

Rapid economic development has occurred in China, and an increasing number of land-based pollutants are being discharged into the Bohai Sea, which have caused tremendous pressure on the marine environment (Li et al. 2015a; Zhuang and Gao 2015; Zhao et al. 2018). The Bohai Sea has a relatively long transport timescale. For example, Wang et al. (2010a) estimated a freshwater residence time of 2.6 years in the 1960s, and a weak upward trend was found in the 1990s. In addition, Liu et al. (2012) calculated a mean age of 3.0 years for Yellow River water within the entire Bohai Sea.

Previous studies have shown that there are significant seasonal variations in the RT within coastal regions when the transport timescales are relatively short (days to months). In these systems, the water particles can be affected by the dynamic forcing only one time or less when transported outward. However, in systems where the transport timescales are much longer than the seasonal timescale, as seen with the Bohai Sea, the water particles can be affected by cyclical forcing (such as monsoon winds or seasonal river discharge) twice or more times when transported outward. Thus, the RT's response to seasonal variations in the hydrodynamics within the Bohai Sea may be different from that in the coastal regions and requires further investigation.

To understand how the RT in the Bohai Sea responds to significant seasonal variations in the hydrodynamics (such as the wind-driven circulation and runoff), this study calculated spatiotemporal variations in the RT of the Bohai Sea using a three-dimensional hydrodynamic model and the adjoint method. The effects of different dynamic factors on the RT were then quantitatively analyzed using numerical experiments to understand the physical mechanisms that prompt RT variations. The remainder of this paper is organized as follows: Section 2 details the configurations of the hydrodynamic model and the residence time model; spatiotemporal variations in the RT of the Bohai Sea are shown in Section 3; the effects of controlling dynamic factors, including wind, tide, river runoff, and baroclinic processes, and the role of monsoon winds on seasonal variations in the RT are discussed in Section 4; and, Section 5 provides a brief conclusion.

## 2 Methodology

### 2.1 Hydrodynamic model

The hydrodynamic model used in this study was established by Guo et al. (2003) and is based on the Princeton Ocean Model (POM) (Mellor 2002). The domain of the model covers the eastern shelf seas of China, including the Bohai Sea, Yellow Sea, and East China Sea (Fig. 1). The horizontal resolution of the model is 1/18°, and there are 21 sigma layers in the vertical direction. The time step of the model was 9 s and 360 s in the external and internal modes, respectively. Climatological monthly mean forcings, including monthly averaged wind, heat flux, rainfall, evaporation, and river runoff, are used (Guo et al. 2003), and tides are prescribed at the open boundaries of the model (Matsumoto et al. 2000). This model has been well validated and previously applied in hydrodynamic studies of the Bohai Sea. As shown by Wang et al. (2008), the model accurately reproduced the four major tidal constituents, and the modeled cotidal chart successfully recreated the observed patterns. Moreover, the modeled seasonal patterns of water

**Table 1** Numerical experiment schemes

| Case | Wind | Tide | Baroclinic process | River runoff |
|---|---|---|---|---|
| 0 | Yes | Yes | Yes | Yes |
| 1 | No | Yes | Yes | Yes |
| 2 | Yes | No | Yes | Yes |
| 3 | Yes | Yes | No | Yes |
| 4 | Yes | Yes | Yes | No |

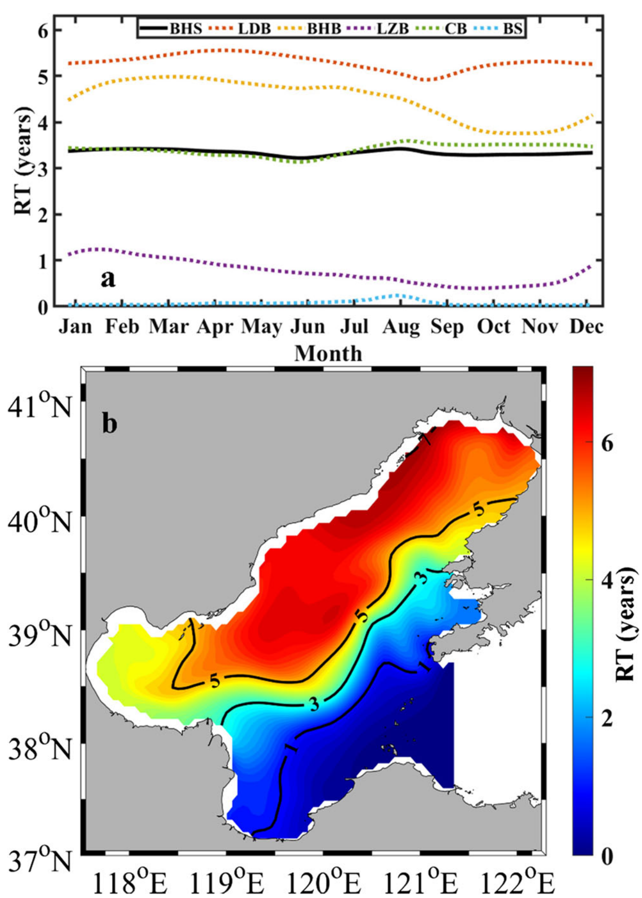


**Fig. 2** **a** Seasonal variations in spatially and vertically averaged RT for the Bohai Sea and sub-bays. The results were treated with a moving average of 15 days to filter out tidal variations. **b** Annual mean RT within the Bohai Sea

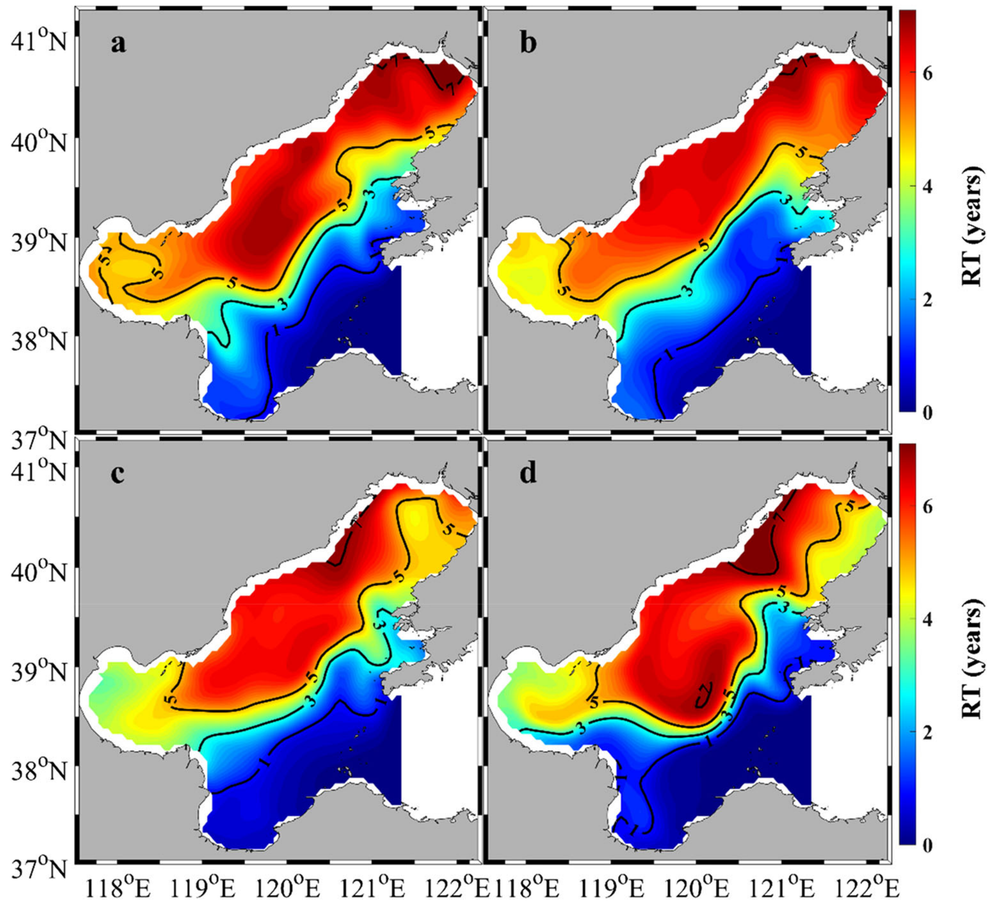


**Fig. 3** Mean RT within the Bohai Sea for the four seasons: **a** Winter, **b** spring, **c** summer, and **d** autumn

temperature and salinity were also consistent with the observed findings. Additionally, Liu et al. (2012) and Li et al. (2017) used this model to estimate the water age of the Yellow River in the Bohai Sea, and analyzed how this was influenced by a water regulation event. Each of these studies indicated that this model could adequately reproduce the hydrodynamic characteristics of the Bohai Sea. Following a 3-year spin-up, the predicted variables of the fourth year were output to drive the RT model of the Bohai Sea.

## 2.2 Residence time model

Based on the concept of RT (Bolin and Rodhe 1973; Takeoka 1984), the adjoint method developed by Delhez et al. (2004) was used to analyze spatiotemporal variations within the RT of the Bohai Sea. The adjoint equation of RT derived by Delhez et al. (2004) is as follows,

$$\frac{\partial \theta}{\partial t} + \delta_{\omega}(\mathbf{X}) + \mathbf{V} \cdot \nabla \theta + \nabla \cdot [\mathbf{K} \cdot \nabla \theta] = 0 \quad (1)$$

where $\omega$ denotes the control region, which includes the entire Bohai Sea bounded by OB1 (the blue dotted line in Fig. 1) in this study, $\theta$ denotes the RT, $\delta_{\omega}(\mathbf{X}) = \{ 1 \;\; \forall \mathbf{X} \in \omega \;\; 0 \;\; \forall \mathbf{X} \notin \omega$ is the characteristic function of the control region $\omega$, $\mathbf{X}$ denotes the position vector, $\mathbf{V}$ is the instantaneous current, and $\mathbf{K}$ is the diffusion coefficient.

The RT diagnosis model established by Lin and Liu et al. (2019a) based on Eq. (1) was used in this study. The RT model is part of the Marine Environment Research and Forecasting (MERF) ocean model (MERF-2.1, Liu et al. 2016; Lin and Liu 2019a, b). The model uses the total variation diminishing advection scheme with alternating limiters (TVDal) and the splitting method to improve accuracy and eliminate numerical dispersion (Lin and Liu 2019b). This RT model has been successfully applied in RT studies in Jiaozhou Bay, Zhuyi Bay, and the eastern shelf seas of China (Cheng et al. 2019; Lin and Liu 2019a; Lin et al. 2020).

The RT model uses the same grids as those of the aforementioned hydrodynamic model of the Bohai Sea.

**Table 2** Seasonal mean RT (units: years) in subdomains of the Bohai Sea

| Subdomains | Annual mean | Winter | Spring | Summer | Autumn |
|---|---|---|---|---|---|
| LDB | 5.28 | 5.53 | 5.54 | 4.97 | 5.08 |
| BHB | 4.12 | 4.50 | 4.43 | 4.00 | 3.55 |
| LZB | 0.72 | 1.02 | 0.82 | 0.51 | 0.54 |
| CB | 3.51 | 3.51 | 3.37 | 3.57 | 3.60 |
| BS | 0.05 | 0.03 | 0.06 | 0.09 | 0.03 |

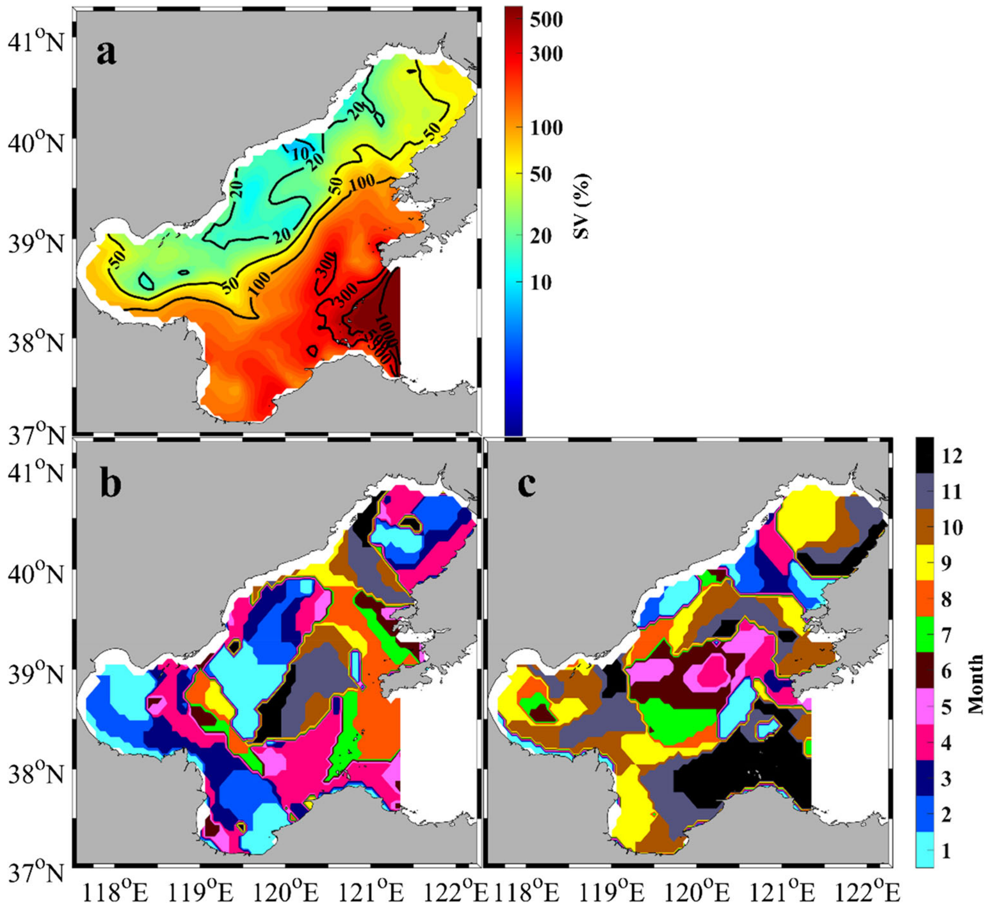


**Fig. 4** **a** SV distribution in the Bohai Sea; **b** and **c** are the months in which the maximum and minimum RT occurred within 1 year, respectively

Hydrodynamic field data (including the water level, three-dimensional flow velocity, and diffusion coefficient) from the hydrodynamic model were used to drive the RT model. It is of note that when using the adjoint method to calculate RT, hydrodynamic field files are input in reverse time (Delhez et al. 2004). In this study, a homogeneous Dirichlet boundary condition ($\theta$=0) was used as the open boundary condition for Eq. (1) at OB1 and the river boundary (Fig. 1). Using this value, the time taken for a water parcel to leave the control region for the first time was determined (Delhez et al. 2004; Delhez 2006; Delhez and Deleersnijder 2006). To improve computational efficiency, OB2 (Fig. 1) was set as the computational boundary of the RT model (i.e., the grids outside of OB2 were not considered during the calculation). The model reached a steady state after 30 years of spin-up, and the results of the 31st year were used to conduct the analyses.

### 2.3 Quantification of the seasonal variation of the RT

An index SV, which denotes the fraction between the range and average of the monthly mean RT in any position, was used to quantify the magnitude of the seasonal variations in the RT within the Bohai Sea, and was calculated as follows:

$$\mathrm{SV}(\mathbf{X}) = \left(\frac{\max(MRT(\mathbf{X}))-\min(MRT(\mathbf{X}))}{mean(MRT(\mathbf{X}))}\right) \times 100\% \quad (2)$$

where $MRT$ denotes the monthly mean RT, and $\mathbf{X}$ denotes the position vector. The SV distribution was used to quantify spatial variations in the magnitude of the seasonal variation in the RT. By comparing the SVs obtained in different experiments, the effects of different dynamic factors on the seasonal variation in the RT in the Bohai Sea were evaluated.

### 2.4 Calculation of Lagrangian residual current

The Lagrangian residual current (LRC) is defined as the net displacement of the labeled water parcel over one or a few tidal cycles divided by the corresponding time interval (Zimmerman 1979). In this study, it is used to explain the spatiotemporal distribution of RT in the Bohai Sea, and the equation for the LRC (Zimmerman 1979; Feng et al. 2008) is as follows,

$$\mathbf{u}_L(\mathbf{X}, \tau; t_0) = \langle \mathbf{u}(\mathbf{X}_0 + \boldsymbol{\xi}(t;\tau)), t; \tau\rangle = \frac{\boldsymbol{\xi}_{nr}}{nT} \quad (3)$$

where $\mathbf{u}_L$ is the LRC; $\mathbf{X}$ denotes the position vector; $t_0$ is the initial time at which the water parcel is tracked; $\mathbf{X}_0$ is the initial

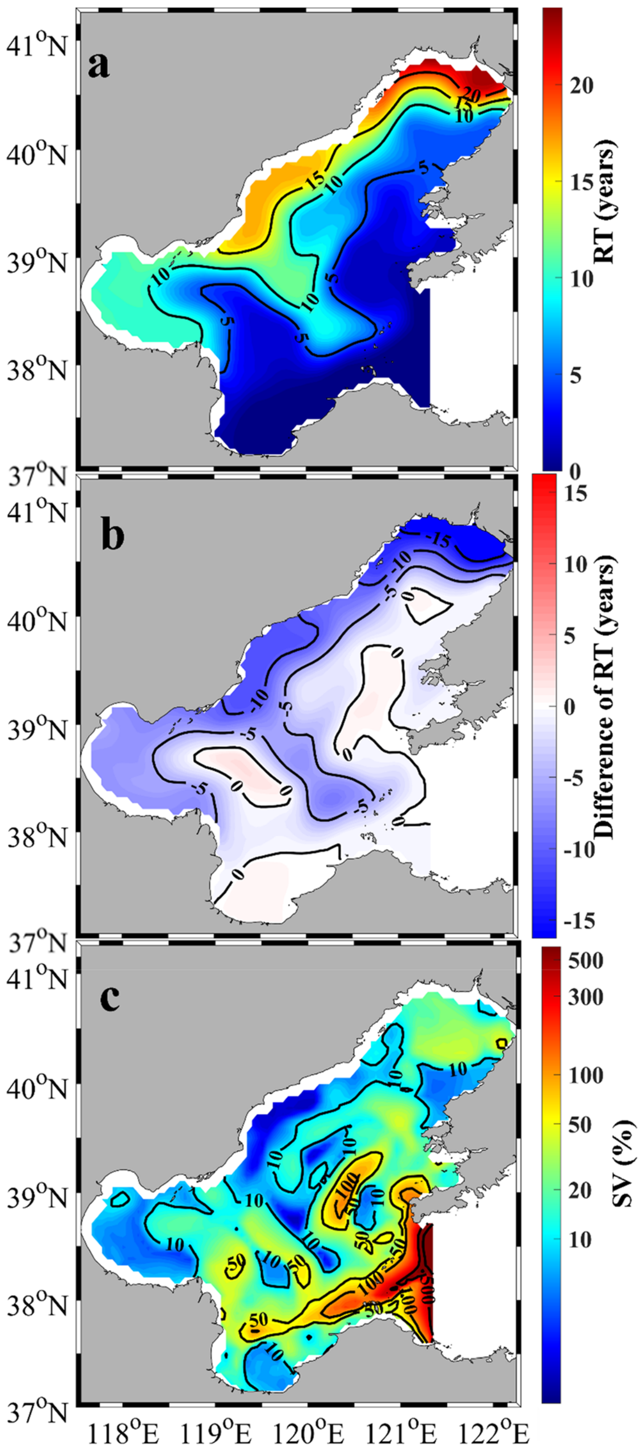


**Fig. 5** **a** Annual mean RT in Case 1; **b** spatial distribution of annual mean $diff_{RT}(1)$ (annual mean RT in Case 0 minus that in Case 1), and **c** SV distribution in Case 1

position vector; $\mathbf{u}(\mathbf{X}_0 + \xi(t;\tau))$ and $\xi(t;\tau)$ are the instantaneous velocity and the displacement of the water parcel, respectively, where $\xi = \mathbf{X} - \mathbf{X_0}$ and $\mathbf{u} = \frac{\partial \xi}{\partial t}$. $\xi_{nr}$ is the net displacement of the water parcel over $n$ tidal cycles; and $T$ is the tidal period.

Based on Eq. (3), we used the particle tracking method to derive the net displacement of particles after 15 days (the least common multiple of the periods of the $M_2$ and $S_2$ tidal constituents, approximately), and we then calculated the LRC by dividing the displacement by 15 days. Particles were released at the center of each of the model's grids in the Bohai Sea every hour throughout the year, and the seasonal mean value of the LRC was used to represent the long-term transport velocity field in winter, spring, summer, and autumn.

### 2.5 Numerical experiment schemes

Numerical sensitivity experiments were designed to assess the impact of the monsoon winds and other dynamic factors (including tides, the baroclinic process, and river runoff) on the RT in the Bohai Sea. The configurations of the numerical experiments are shown in Table 1. Case 0 was the control run that considered all dynamic factors (wind, tide, baroclinic processes, and river runoff) in the model. In Case 1, the wind speed in the hydrodynamic model was set to 0 m/s, and RT was calculated using the new dynamic field to assess the impact of monsoon winds on the RT. In Case 2, tidal forcing was removed from the open boundary in the hydrodynamic model, and the RT was calculated using the no-tide hydrodynamic field. In Case 3, the seawater temperature and salinity were set to constant values (temperature of 10 °C, salinity of 35 psu). Lastly, in Case 4, all of the river runoff inputs to the Bohai Sea (including the Yellow River, Haihe River, and Liaohe River) were removed from the hydrodynamic model.

## 3 Results

The model results showed that the annual mean of the spatially and vertically averaged RT within the entire Bohai Sea is 3.43 years. The longest and shortest were 3.57 years and 3.33 years in winter and autumn, respectively, which suggests that the seasonal variation in the RT averaged over the entire Bohai Sea is not obvious (~ 7%). The annual mean RT was close to the estimated value based on the observation data. For example, Wang et al. (2010a) used a box model based on the freshwater fraction method to estimate an RT of 2.6 years in the Bohai Sea. Liu et al. (2017) estimated that the RT within the Bohai Sea was 1.7 ± 0.8 years by a $^{226}Ra/^{228}Ra$ mass balance model. It is of note, however, that box models usually overestimate the exchange rate of the system and thus underestimate RT (Yang et al. 2012). Therefore, the hydrodynamic and RT models were believed to be reliable for use in this study.

The results showed evident regional and temporal variations in RT within the Bohai Sea (Figs. 2 and 3). There was an increase in the annual mean RT from the BS to the northwest coast, with higher values of RT in the center and

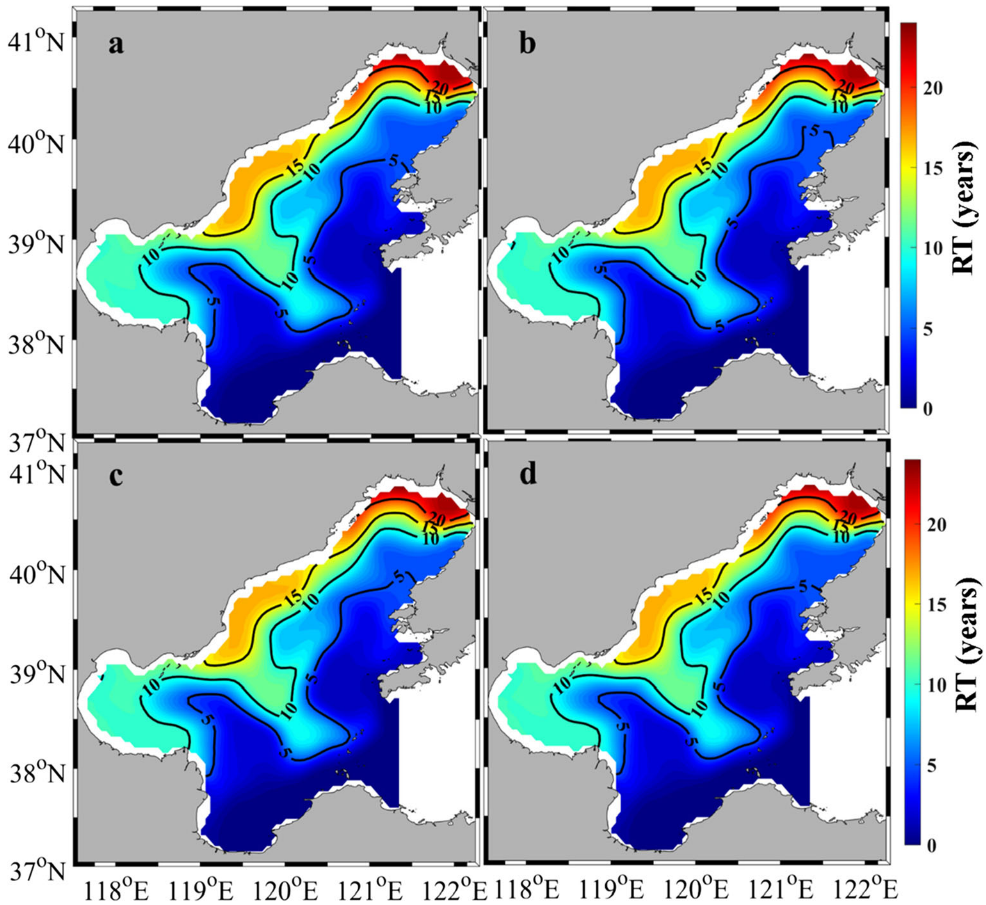


**Fig. 6** Mean RT within the Bohai Sea for the four seasons: **a** Winter, **b** spring, **c** summer, and **d** autumn for Case 1

northwest of the Bohai Sea (Fig. 2b). The annual means of the spatially and vertically averaged RT were 0.05, 0.72, 3.51, 4.12, and 5.28 years in the BS, LZB, CB, BHB, and LDB, respectively (Table 2). Although the seasonal variation of the spatially mean RT was not obvious, there were significant differences in the spatial pattern of RT within the Bohai Sea during the four seasons (Figs. 2a and 3). The value of RT was much higher in winter and autumn in the center of CB (~ 6 years). The longest RT (> 7 years) appeared in the northwestern part of the LDB in winter and the bay mouth of LDB in autumn (Fig. 3a, d). The shortest RT appeared in summer in LZB (< 1 year) (Fig. 3c), and in autumn in the southern part of BHB (~ 2 years) (Fig. 3d).

**Table 3** Mean SV (units: %) within the Bohai Sea for different cases

| Subdomains | Case 0 | Case 1 | Case 2 | Case 3 | Case 4 |
|---|---|---|---|---|---|
| Bohai Sea | 292.86 | 87.36 | 123.37 | 359.61 | 232.37 |
| LDB | 43.90 | 15.40 | 55.12 | 64.00 | 39.94 |
| BHB | 50.14 | 13.45 | 103.72 | 30.12 | 21.68 |
| LZB | 162.86 | 22.68 | 165.81 | 100.91 | 76.29 |
| CB | 143.53 | 33.45 | 95.07 | 170.55 | 131.08 |
| BS | 1937.73 | 647.95 | 397.80 | 2489.88 | 1472.93 |

The SV results showed an increase in the seasonal variation from northwest to southeast in the Bohai Sea (Fig. 4a). It was less than 100% in the western Bohai Sea (including the whole LDB, BHB, and the western CB), and more than 300% in the eastern part of CB; even reaching 1000% in the BS. The annual mean of spatially and vertically averaged SV was approximately 300% over the entire Bohai Sea, which suggests a significant seasonal variation in RT within the Bohai Sea.

From the results above, the seasons and months in which the spatially and vertically averaged RT were highest and lowest differed across the various subregions (Fig. 4b, c, and Table 2). In the coastal regions, the highest value appeared in winter or spring (Table 2): it occurred in January or February in BHB, LZB, the center of LDB, and the western part of CB (Fig. 4b), and in April in the east of LDB, the southern part of LZB and CB. The lowest value appeared in summer or autumn (Table 2); for example, the RT was lowest in September in the western part of LDB, BHB, and LZB, in October, or November in the eastern part of those regions (Fig. 4c). Whereas in the center of CB, the value was the lowest in spring (April, May, or June), and the highest in autumn (Fig. 4b, c). In the BS, the maximum RT in the northern (southern) occurred in August (April), with the minimum appearing in December (Fig. 4b, c). These results provided evidence of strong regional differences in RT variations throughout the

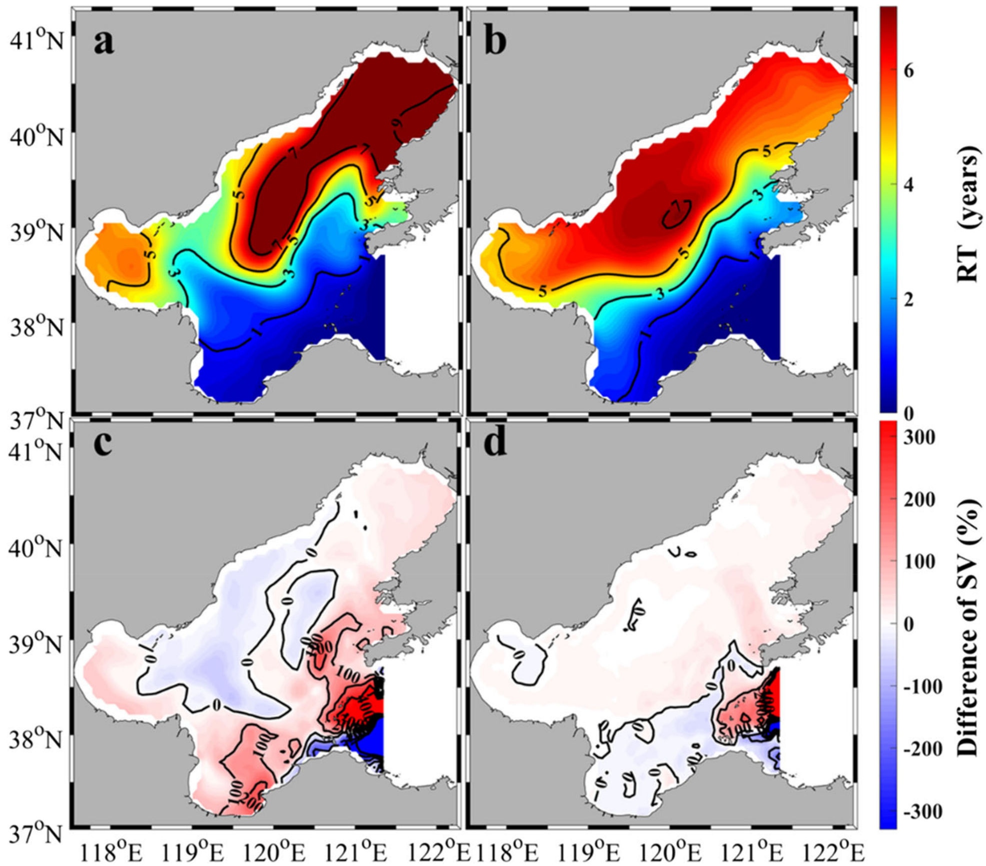


**Fig. 7** Annual mean RT in the Bohai Sea in (**a**) Case E1, (**b**) Case E2. Spatial distribution of (**c**) $diff_{SV}(E1)$ and (**d**) $diff_{SV}(E2)$

Bohai Sea, implying that environmental management policies could be tailored to local conditions.

## 4 Discussion

### 4.1 Influence of dynamic factors on the RT of the Bohai Sea

Winds, tides, river runoff, and baroclinic processes affect the hydrodynamics and transport timescales of coastal oceans (Yuan et al. 2007; Wang et al. 2008; Wang et al. 2010b; Cai et al. 2014; Sun et al. 2014; Li et al. 2015b; Du and Shen 2016; Lin et al. 2020; Ju et al. 2020). To understand their influences on the RT of the Bohai Sea, we conducted four sensitivity experiments and then discussed the influences of the different dynamic factors.

#### 4.1.1 Wind

Compared to the control run, the spatial pattern of the annual mean RT in Case 1 also shows an increase from the BS to the northwest coast, but the value is much higher (Fig. 5a). The annual mean RT in the northwest and LDB increases to more than 10 years and 20 years, respectively, and is approximately 200% of that in Case 0. The annual mean of the spatially and vertically averaged RT within the Bohai Sea increases by approximately 90% after removing the wind from the hydrodynamic model. There are increases of 230.34% in BS, 109.40% in BHB, and 101.85% in LDB (Fig. 5a). In this paper, two indexes $diff_{RT}(i)$ and $diff_{SV}(i)$ were used to reflect the differences in RT and SV between cases i and Case 0, which was calculated as follows,

$$diff_{RT}(i) = RT_{\text{Case }0} - RT_{\text{Case }i} \quad (i = 1, 2, 3, 4, E1, E2, \ldots E7) \tag{4}$$

$$diff_{SV}(i) = SV_{\text{Case }0} - SV_{\text{Case }i} \quad (i = 1, 2, 3, 4, E1, E2, \ldots E7) \tag{5}$$

The spatial distribution of annual mean $diff_{RT}(1)$ (Fig. 5b) shows that monsoon winds decrease the RT in most regions of the Bohai Sea.

The spatial patterns of the seasonal RT across the four seasons are very similar to each other in Case 1 (Fig. 6), which suggests that there is a significant decrease in SV throughout the entire Bohai Sea in Case 1. In most areas of the Bohai Sea, the SV is less than 20% (as shown in Fig. 5c), although it is more than 100% in regions near the BS, and approximately 50% in the east of the CB (this value was approximately 200% in Case 0). The average SV in the Bohai Sea of Case 1 was

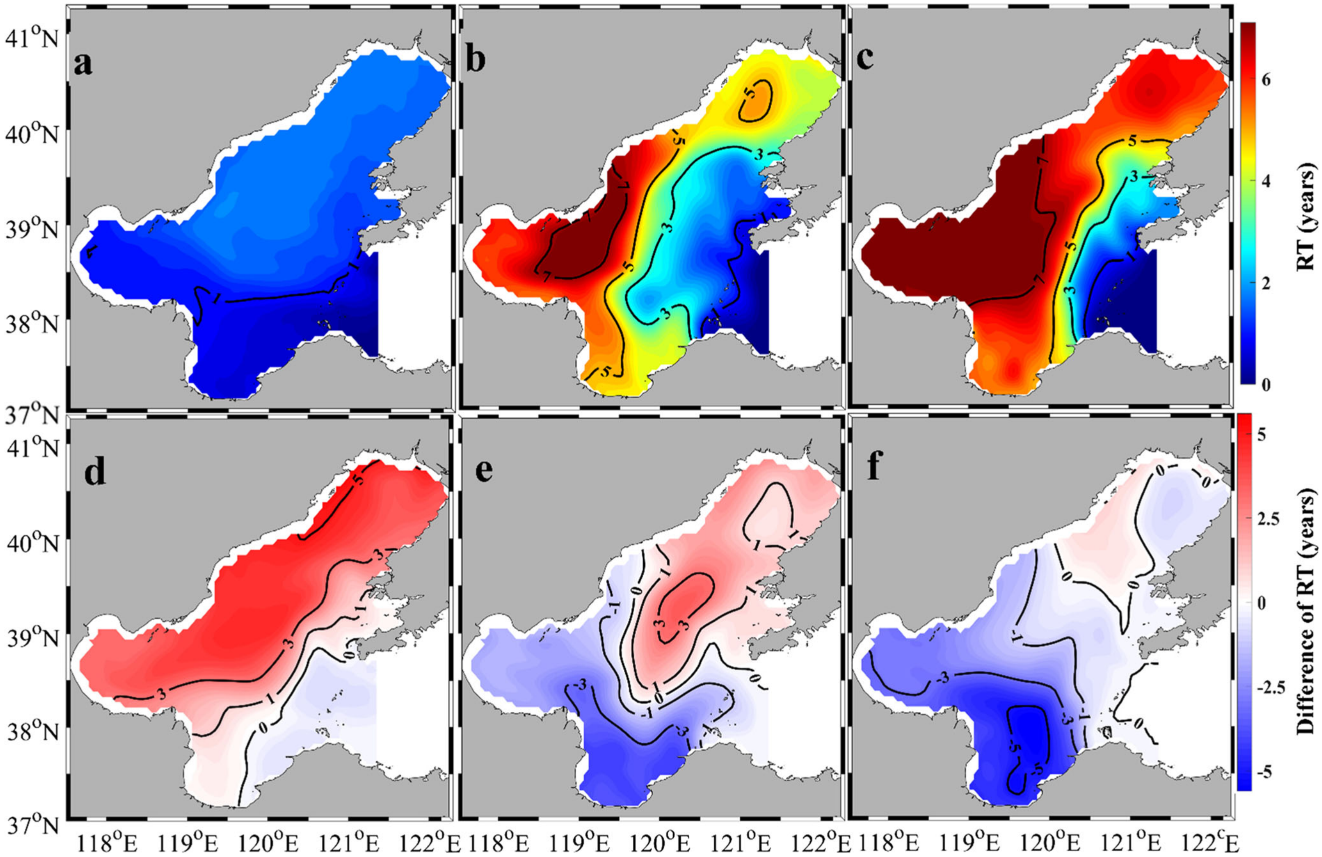


**Fig. 8** Annual mean RT in the Bohai Sea in (**a**) Case 2, (**b**) Case 3, and (**c**) Case 4. Spatial distribution of annual mean (**d**) $diff_{RT}(2)$, (**e**) $diff_{RT}(3)$, and (**f**) $diff_{RT}(4)$

87.36%, which is much less than that in Case 0 (only approximately 30% of that in Case 0) (Table 3). The SVs in each subregion also decrease significantly in Case 1 and are only 15–35% of those in Case 0 (Table 3). These results imply that monsoon winds can reduce the RT and facilitate water exchange in the Bohai Sea, and monsoon winds play an important role in the seasonal variation of RT in the Bohai Sea.

Previous studies have shown that both local and remote winds could affect the water exchange processes in the coastal regions (Jordi et al. 2011; Mitarai et al. 2009; Shen and Gong 2009; Wang and Elliott 1978). Thus, two additional experiments (Cases E1 and E2) were designed to quantify the relative importance of local (i.e., from within the Bohai Sea) and remote (i.e., from the Yellow Sea and East China Sea (ECS)) winds in controlling the RT of the Bohai Sea. In Case E1, the local winds from within the Bohai Sea were removed from the hydrodynamic model; in E2, the winds from the Yellow Sea and ECS were removed. The RT in these two cases was then

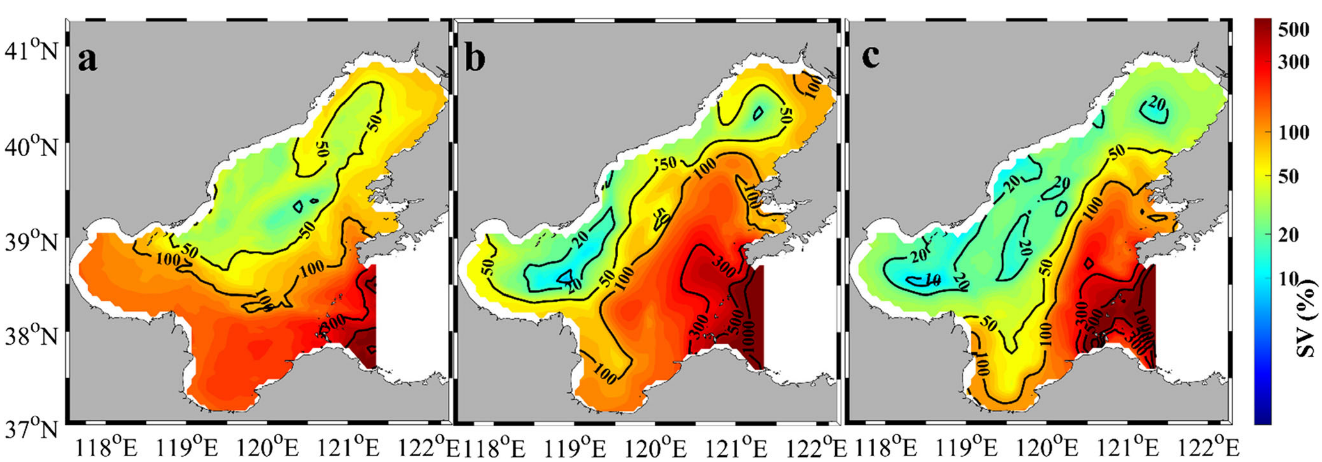


**Fig. 9** SV distribution in (**a**) Case 2, (**b**) Case 3, and (**c**) Case 4

calculated using the adjusted hydrodynamic data. The results show that the RT value within the Bohai Sea increased significantly in Case E1, especially in the LDB and north of the CB (Fig. 7a). The $diff_{SV}(E1)$ shows an obvious increase in the LZB and eastern CB (Fig. 7c); however, the RT and SV observed in Case E2 are similar to those in Case 0 (Fig. 7b, d). Therefore, the effects of local winds on the RT in the Bohai Sea are shown to be much stronger than those of the remote winds, with local winds playing a more dominant role in the seasonal variation of the RT as well.

### 4.1.2 Tide

The value of RT decreased significantly in most areas of the Bohai Sea when tides were excluded from the hydrodynamic model in Case 2 (Fig. 8a). The annual mean of the spatially and vertically averaged RT for the entire Bohai Sea was reduced to 1.21 years, a decrease of 64.75% compared to Case 0. Tides can reduce the coastal circulation in shelf seas by intensifying bottom friction and thus increase shelf water RT (Lin et al. 2020). The spatial pattern of annual mean $diff_{RT}(2)$ (Fig. 8d), which can reflect the effect of tides on the RT, is similar to the RT spatial patterning seen in Case 0. Thus, we can conclude that tides could be the primary factor determining the spatial distribution of the annual mean RT in the Bohai Sea.

Although the mean SV decreased to 123.37% in Case 2 (about 40% of that in Case 0), there are significant regional differences in the Bohai Sea. The SV is more than 50% in the entire Bohai Sea and approximately 300% in the BS when tides are removed from the hydrodynamic model in Case 2 (Fig. 9a). Compared to the control run, the SV in Case 2 increased by approximately 100% in the BHB but decreased by 80% in the BS (Table 3). However, the SV in Case 2 is similar to that of Case 0 in the other regions. These results suggest a significant regional difference in the effect of tides on the seasonal variations of RT in the Bohai Sea.

### 4.1.3 Baroclinic processes

The baroclinic processes can affect the hydrodynamic field in coastal waters, particularly near estuaries, and thus has an impact on the water exchange (Wang et al. 2010b; Cai et al. 2014; Du et al. 2018). When the baroclinic processes were removed, the mean RT within the entire Bohai Sea was 3.70 years. The RT pattern in Case 3 differs from Case 0, especially in regions near the Yellow River estuary and the central CB (Fig. 8b), which indicates that the baroclinic processes have a significant effect on the RT in these regions. The spatial pattern of annual mean $diff_{RT}(3)$ shows that the impact of the baroclinic process varies between regions: the RT increases (decreases) in the north (south) of the Bohai Sea (Fig. 8e).

The SV pattern in Case 3 is similar to that of the control run (Fig. 9b), even though there is a local difference near the estuary. It should be noted that the baroclinic effect is more important for ocean circulation in summer than in the other seasons, and the effect of the baroclinic processes on the RT in spring and summer is also slightly stronger than that in the

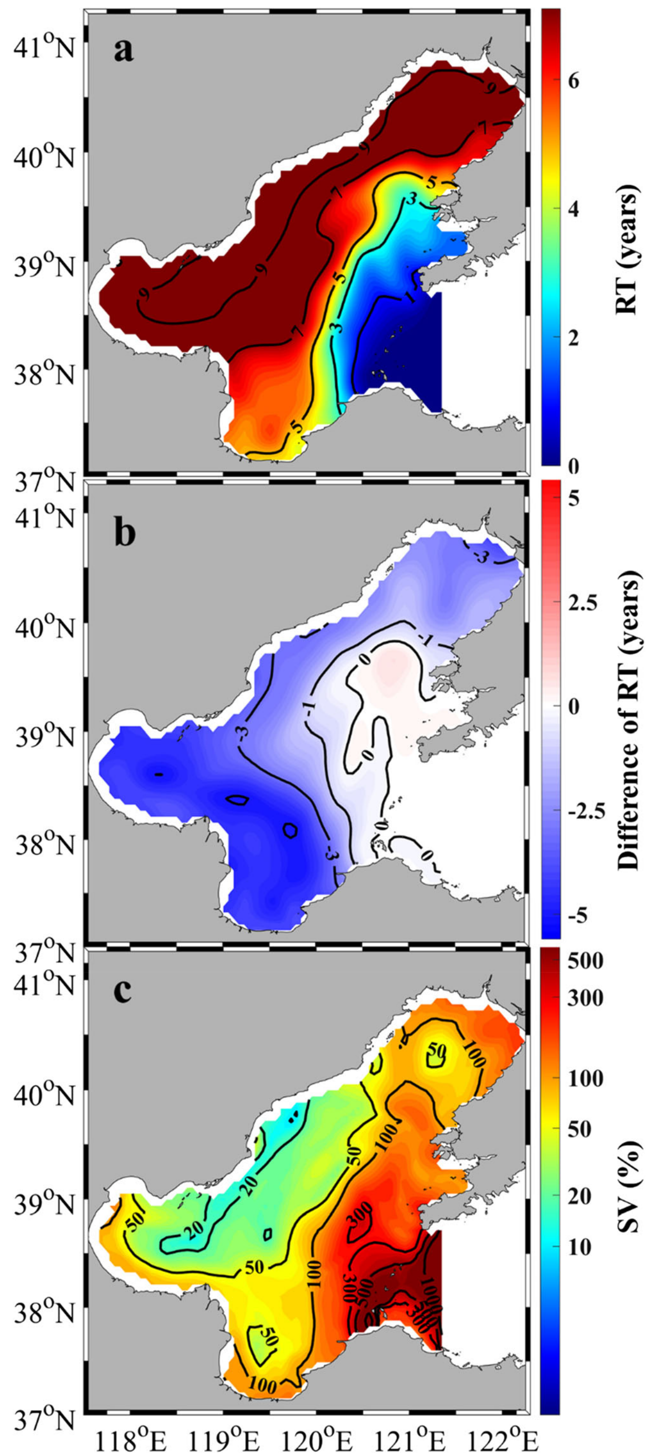


**Fig. 10** **a** Annual mean RT in Case E3; **b** Spatial distribution of annual mean $diff_{RT}(E3)$, and **c** the SV distribution in Case E3

autumn and winter. However, when compared to the wind effect, the baroclinic effect on the SV of the RT in the Bohai Sea is relatively weak. Therefore, baroclinity is likely not the main factor controlling the SV of RT within the Bohai Sea.

#### 4.1.4 River runoff

Freshwater discharge intensifies the flushing of estuaries and coastal waters, thereby enhancing water exchange (Wang et al. 2010b; Du and Shen 2016). The effect of river runoff on the hydrodynamics and RT consists of the baroclinic and barotropic components. The baroclinic component is mainly induced by the effect of river runoff on salinity levels. To distinguish the effect of river runoff and the baroclinic processes on the RT in the Bohai Sea, an additional case (Case E3) was added in which the salinity was held constant throughout the entire Bohai Sea to exclude the baroclinic effects induced by the river plume.

When river runoff was removed from the hydrodynamic model (Case 4), the mean RT of the entire Bohai Sea is 4.91 years. The pattern of RT in Case 4 is similar to that in Case 3; however, the RT is much longer, particularly in regions near the Yellow River estuary (Fig. 8c). The spatial distribution of annual mean $diff_{RT}(4)$ shows that river runoff decreases the RT by ~ 5 years in the south of the Bohai Sea, especially in the LZB (Fig. 8f). The $diff_{RT}(E3)$ likely reflects the effect of the baroclinic processes of river runoff on the RT. As shown in Fig. 10b, the baroclinic process of river runoff significantly decreases the RT by more than 3 years in the estuarine regions of the BHB, LDB, and LZB. Both Case E3 (Fig. 10) and Case 4 (Fig. 8c, f, Fig. 9c) suggest that the baroclinic processes resulting from river runoff plays a dominant role in the effect of river runoff on the RT in the Bohai Sea.

In addition, Case 4 shows an obvious decrease in the SV of the RT near estuaries, especially near the Yellow River (Fig. 9c), and it decreases by approximately 50% in LZB and BHB, respectively. However, the SVs of the other subregions are very similar to those in Case 0. These results indicate that the effect of river runoff on SV also has regional variations, especially near the Yellow River.

### 4.2 Impact of monsoon winds on RT seasonal variability

The above results indicate that the winds are the main controlling factor determining the seasonal variation in RT within the Bohai Sea. The RT reflects the long-term transport timescale, and its value and spatiotemporal distribution depend on the hydrodynamic field within the control region (Liu et al. 2004;

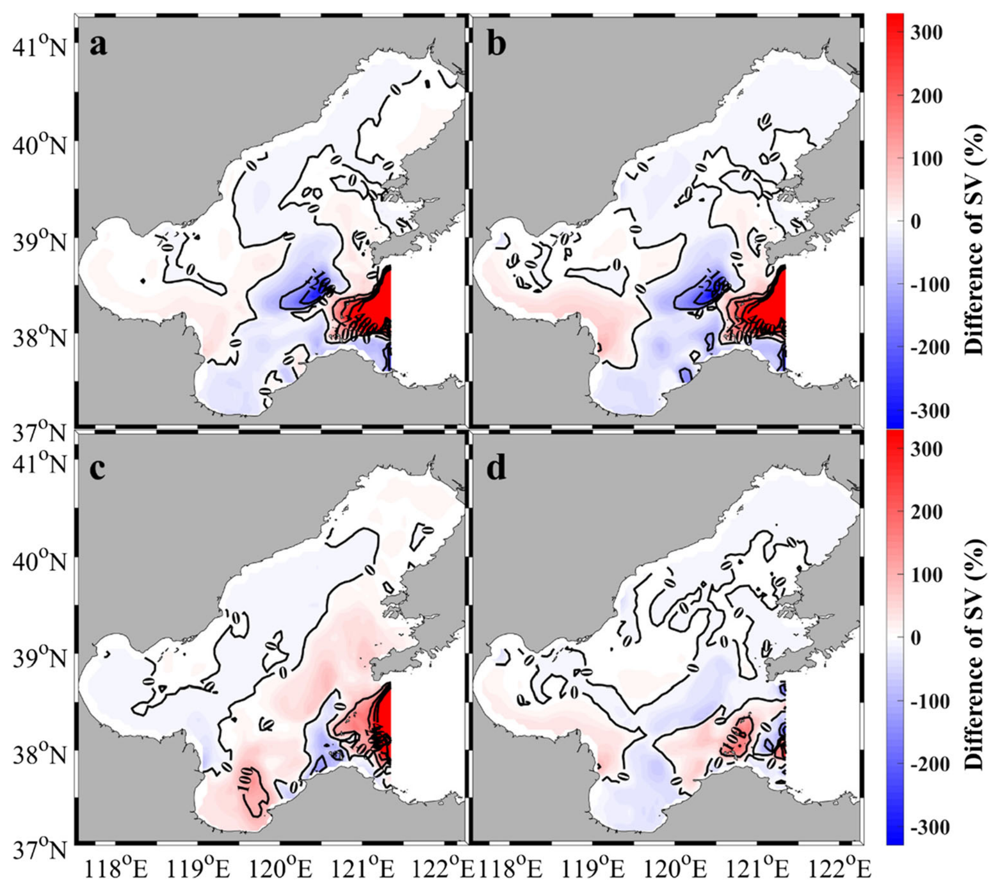


**Fig. 11** Spatial distribution of (**a**) $diff_{SV}(E4)$, (**b**) $diff_{SV}(E5)$, (**c**) $diff_{SV}(E6)$, and (**d**) $diff_{SV}(E7)$

Du and Shen 2016). Water transport is controlled by the advection and diffusion processes from Eq. (1). Therefore, we used an index, the Péclet number, to quantify the relative importance of each process in controlling RT within the Bohai Sea. The Péclet number (Pe) is defined as the ratio of horizontal advection to diffusion (Guyon et al. 2001; Jenkins 2003; Patankar 1980), and the equation is as follows,

$$Pe = \frac{vL_{\text{char}}}{D} = \frac{\text{horizontal advection transport}}{\text{horizontal diffusion transport}} \quad (6)$$

where $v$ is the residual velocity, $L_{\text{char}}$ is the characteristic length of the research domain, and $D$ is the horizontal diffusion rate. In the Bohai Sea, $v$ is $\sim 10^{-2}\ m/s$, $L_{\text{char}}$ is $\sim 10^{5}\ m$, and $D$ is $\sim 10^{2}\ m^2/s$ from the hydrodynamic model. Thus, Pe in the Bohai Sea is $\sim 10$, which means that the effect of horizontal advection on the RT is approximately one order of magnitude greater than that of the diffusion. An added experiment excluding horizontal diffusion from the model further confirms its negligible effect on the RT. Furthermore, four additional experiments were included to quantify the effect of the change in vertical diffusion induced by the winds, tides, baroclinic processes, and river runoff, (Cases E4–E7, respectively). The experiments were calculated using the same variables as Case 0 save for the vertical diffusion values from Cases 1–4, respectively. The RT and SV within the Bohai Sea were calculated using the adjusted hydrodynamic data from each case. $Diff_{SV}(E4) - (E7)$ are shown in Fig. 11, and they are relatively smaller than $diff_{SV}(1) - (4)$. Which suggests that the effect of the change in the vertical diffusion induced by the dynamic factors is much weaker than that of the change in the advection. As mentioned in Section 4.1, the wind is the main factor controlling the SV in RT within the Bohai Sea. Thus, we can conclude that the effect of winds on the RT is mainly related to the effect of winds on the currents. In addition, long-term transport in a tidally dominated system is highly related to the residual current, and many studies have suggested that the LRC is related to long-term transport in a macro-tidal system (Feng et al. 1986, 2008; Jiang and Feng 2011, 2014). Thus, we further analyzed seasonal variations in the LRC and the effect of winds on the LRC in the Bohai Sea.

Significant seasonal variations in the LRC (Fig. 12) were found within the Bohai Sea, and this result is consistent with those of previous studies (Wei et al. 2001, 2004; Wang et al. 2010b; Zhou et al. 2017; Guo et al. 2018). As shown in Fig. 12a, the speed of the LRC is much lower in the center than in the coastal regions of the Bohai Sea in winter. Water in the eastern/southwestern areas flows to the southwestern/southeastern area of the Bohai Sea, and only water near the

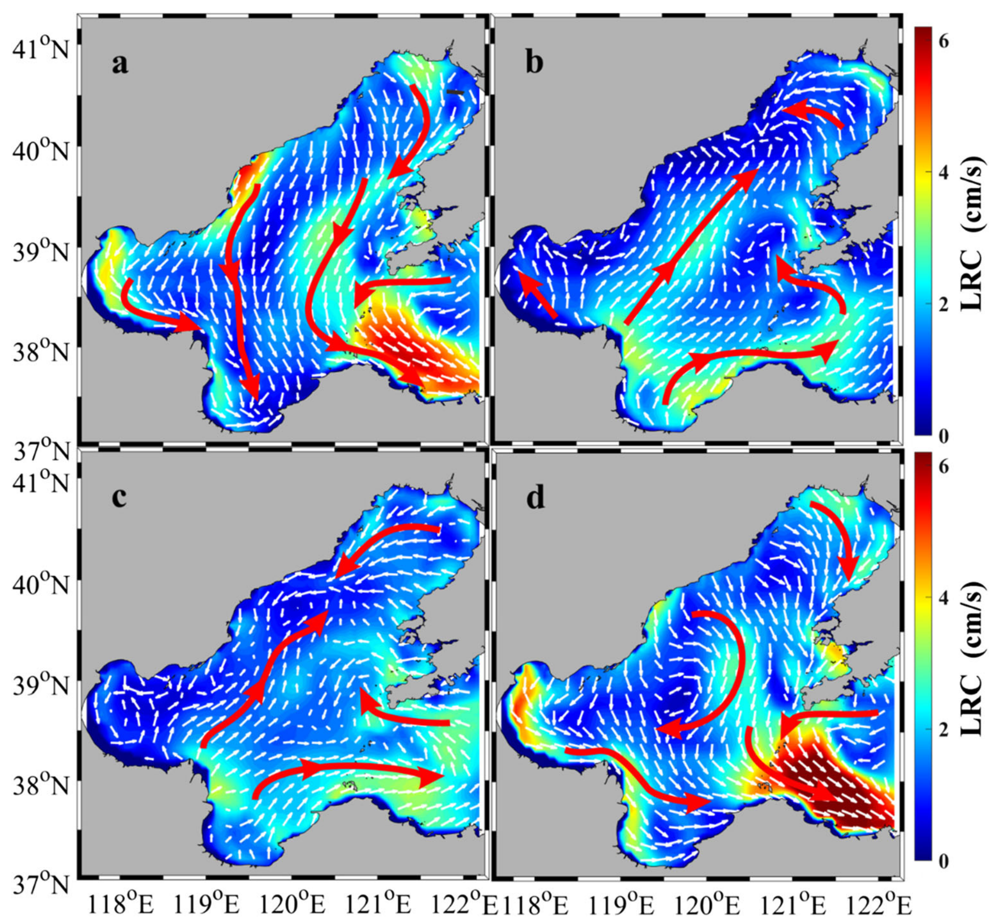


**Fig. 12** Lagrange residual currents (white arrows) in (**a**) winter, (**b**) spring, (**c**) summer, and (**d**) autumn. The colors show the patterns of the LRC speed (cm/s)

BS is transported out of the Bohai Sea. In spring and summer, there is an evident decrease in the speed of the LRC, which is lower in the BHB and on the west coast but higher in the LZB and the center of the Bohai Sea (Fig. 12b, c). In the southern Bohai Sea, the LRC flows to the northeast but moves south in the western LDB. In addition, water in the LZB and near the BS can be transported out of the Bohai Sea. In autumn, the LRC in the Bohai Sea is similar to that in winter, except for regions in the center of the CB, where there is a residual current vortex (Fig. 12d), and water in the BHB and LZB can be transported out of the Bohai Sea.

These seasonal variations in the LRC induce significant differences in the transport pathways of water parcels released in different seasons, which results in seasonal variations in the RT within the Bohai Sea. However, compared with the spatial distribution of RT, there is spatial consistency between the lower/higher speed of the LRC and higher/lower RT values (for example, in the top and central areas of the LDB and the central/western areas of the CB) (Fig. 3). As shown by the trajectory of typical particle tracking in Fig. 13, particles released in the central CB are transported to the west in the autumn, remain in the LZB for more than 1 year in winter, and move out of the Bohai Sea through the southern BS in summer. Thus, the RT in the CB is longer in autumn and winter. In the BHB, the particles released in the autumn are more easily transported to the LZB and out of the Bohai Sea, while they spend more time in the BHB and LZB in the other seasons. Hence, the RT of the BHB is relatively short in autumn. Particles released in the LDB remain there for more time in the spring and elsewhere in the Bohai Sea in winter, while they are more likely to be transported out of the Bohai Sea in the summer and autumn. Therefore, the longer RT of the LDB occurs in the winter and spring. In conclusion, the LRC appears to be the main factor controlling the RT and its SV within the Bohai Sea.

Seasonal variations in the LRC are mainly induced by the monsoon winds, as demonstrated by the results of Case 1: the patterns and directions of the LRC in the Bohai Sea are very

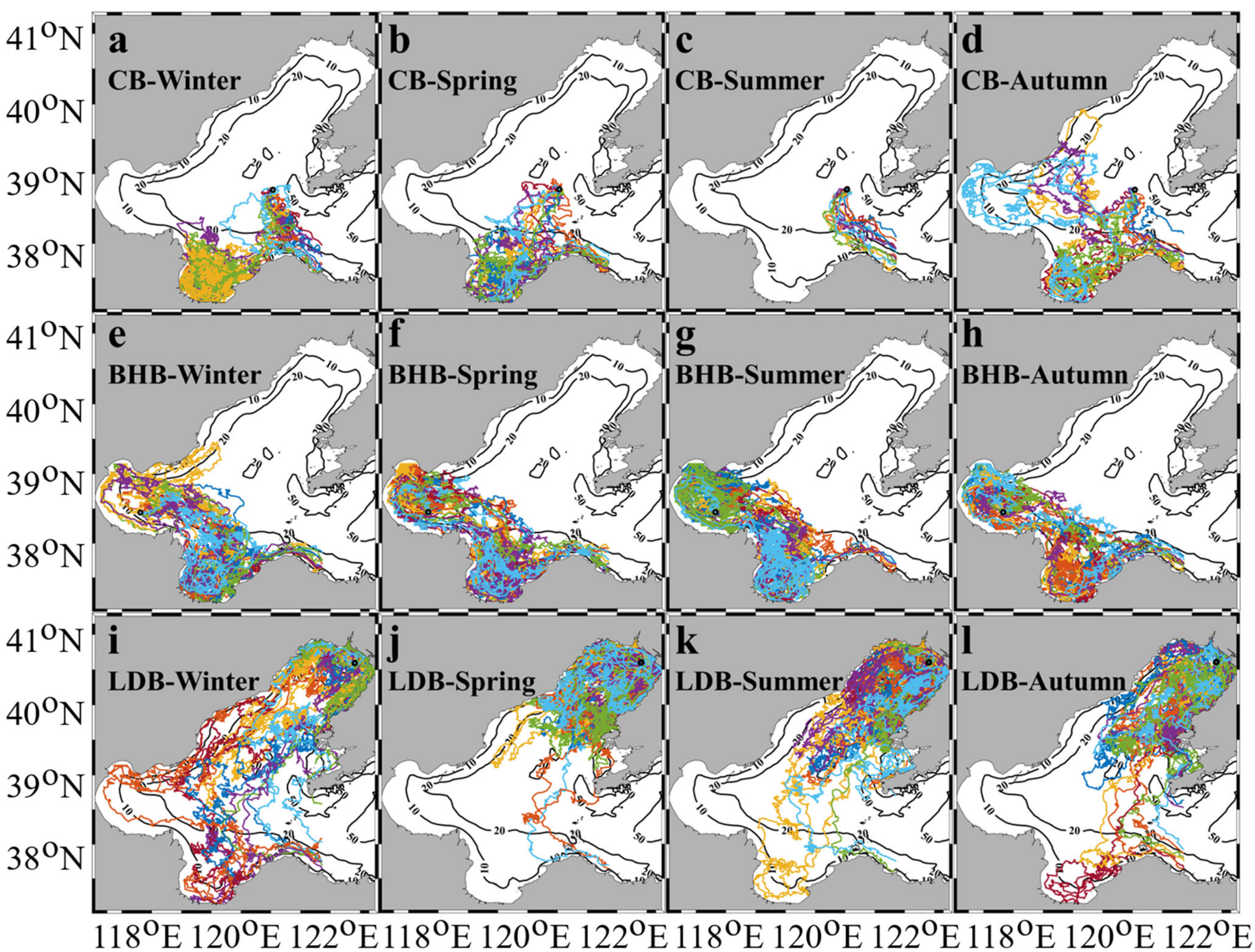


**Fig. 13** Particles trajectories released in CB, BHB, and LDB in four seasons (the color of lines show the trajectories of different particles released at the same point)

similar in all four seasons (Fig. 14). Therefore, water parcels released in the same location in different seasons have similar fates, and this explains the disappearance of seasonal RT variations when winds have been removed. The LRC is also weakened considerably when monsoon winds have been removed from the hydrodynamic model. The average velocity of the LRC in the four seasons in Case 1 was ~ $4.9 \times 10^{-3}$ m/s, which is approximately half the value of the control run. It is thus difficult for the water masses in most of the interior regions of the Bohai Sea to be transported to the strait and out of the Bohai Sea when the monsoon winds have been removed, which means that RT has higher values in Case 1 (Fig. 5).

The wind-induced residual current (Fig. 15e–h), which was calculated using the LRC in Case 0 minus that in Case 1, is similar to the LRC in the Bohai Sea during the four seasons. This suggests that the wind-induced residual current plays a dominant role in the LRC. Therefore, significant variations in the LRC should be related to the wind-induced residual current and thus to the seasonal shift in the wind direction. In the center of the Bohai Sea, the wind-induced residual current is mainly affected by the wind because of the smooth topography (Huang et al. 1999; Deng and Zhao 2020). The direction of water transport is related to the wind direction, water depth, and Ekman layer thickness ($\pi\sqrt{\frac{2Av}{|f|}}$, where $Av$ is the vertical viscosity and $f$ is the Coriolis parameter) (Monismith 1986; Huang et al. 1999; Pfeiffer-Herbert et al. 2015; Deng and Zhao 2020). According to Ekman theory, if the water is deep enough, wind-driven transport is oriented perpendicular to the wind (Ekman 1905), whereas if the water is shallow and less than half the Ekman layer thickness, the wind-driven transport direction is basically consistent with that of the wind direction (e.g., Estrade et al. 2008). In winter and autumn, due to strong winds and surface cooling, the water is well mixed in the vertical direction, and the $Av$ is of the order of $10^{-2}$ m$^2$/s and $f$ approximately $10^{-4}$ rad/s from the hydrodynamic model. The Ekman layer thickness is thus more than 40 m and much larger than the mean water depth (~ 18 m) of the Bohai Sea. Therefore, the wind-induced residual current flows to the southwest along the wind direction, especially in the center of the Bohai Sea (Fig. 15e, h). However, under the effect of the north wind and modulation of the shoreline, the wind-induced residual current flows to the east in the nearshore regions. In spring and summer, stratification is strengthened, and the vertical viscosity is weakened ($Av$ ~ $10^{-3}$ m$^2$/s), and the Ekman layer thickness decreases to approximately 15 m, which is shallower than the mean water depth. Therefore, the wind-induced residual current is oriented perpendicular to the wind and flows to the northeast within the Bohai Sea

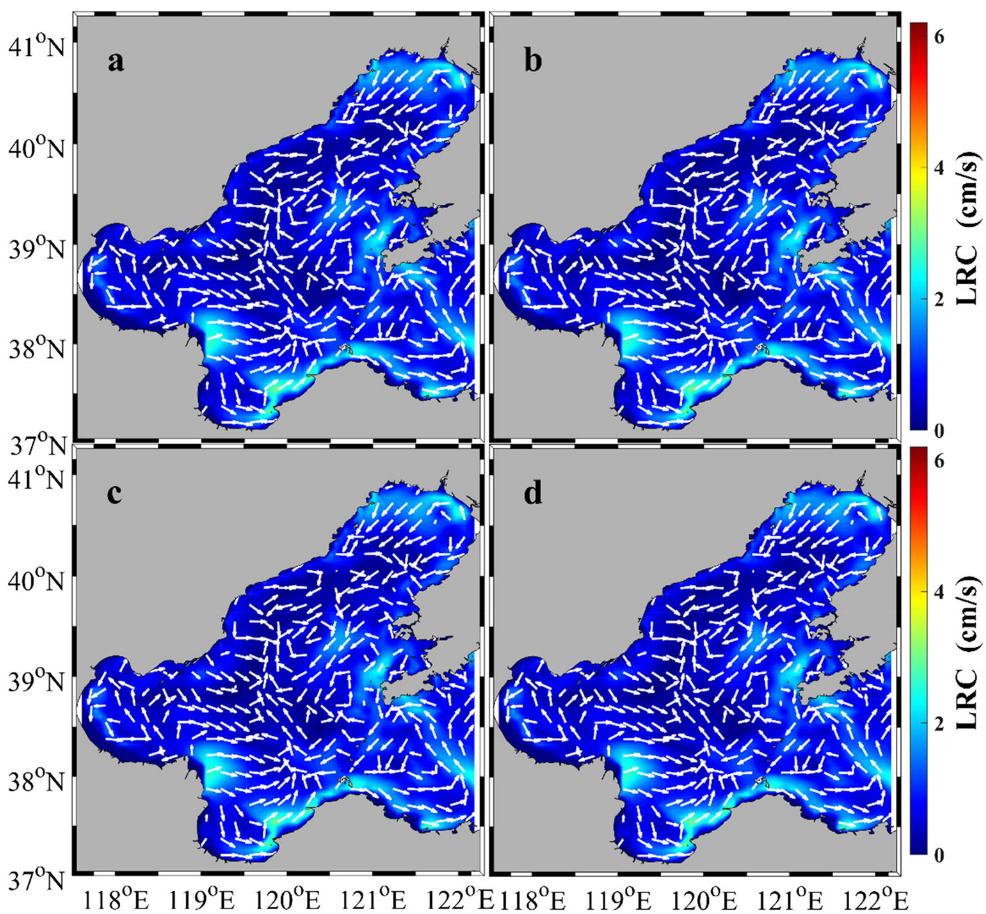


**Fig. 14** Lagrange residual currents (white arrows) in (**a**) winter, (**b**) spring, (**c**) summer, and (**d**) autumn for Case 1. The colors show the patterns of the LRC speed (cm/s)

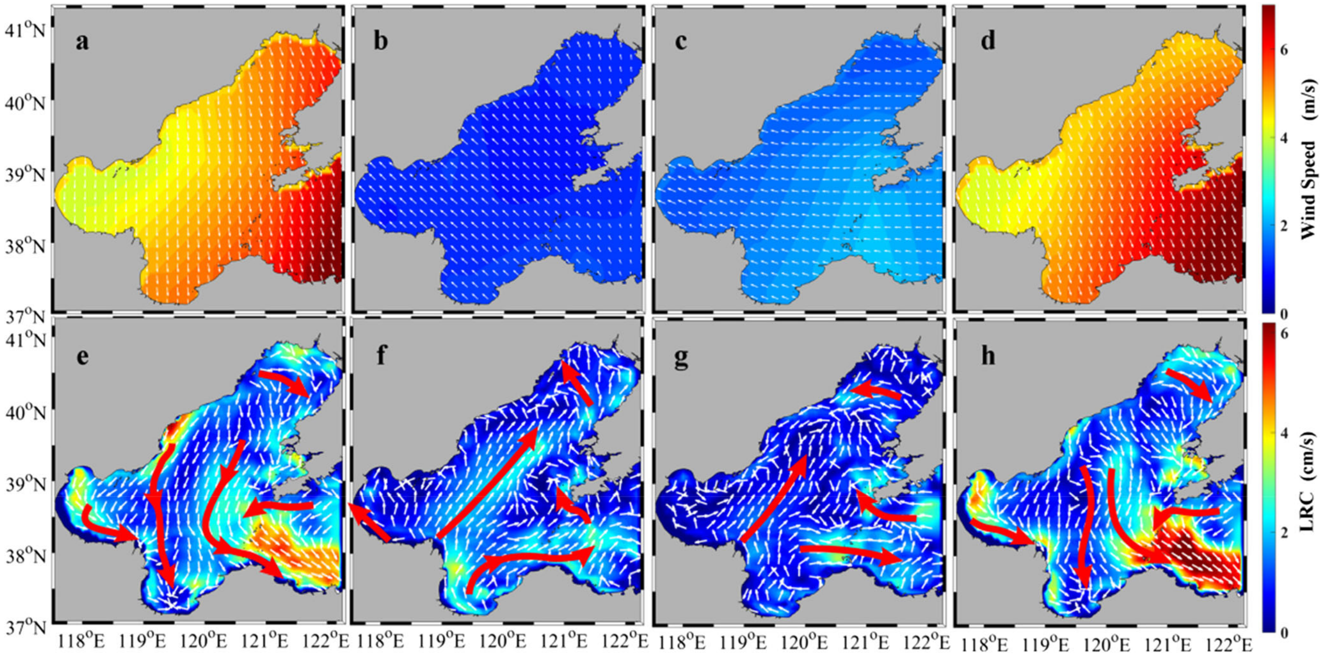


**Fig. 15** Wind field used in the hydrodynamic model in (**a**) winter, (**b**) spring, (**c**) summer, and (**d**) autumn. The colors show the patterns of the wind speed (m/s). The wind-induced residual current (LRC in Case 0 minus that in Case 1) in (**e**) winter, (**f**) spring, (**g**) summer, and (**h**) autumn. The colors show the patterns of the wind-induced residual current speed (cm/s)

(Fig. 15f, g). By driving the shift of the wind-induced residual current, the monsoon winds cause seasonal variations in the LRC within the Bohai Sea and thus induce significant seasonal RT variability.

## 5 Conclusions

This study used a 3-D hydrodynamic model with the adjoint method of RT to investigate the RT of water in the Bohai Sea and its seasonal variations. The model results show that the annual mean spatially averaged RT in the entire Bohai Sea is 3.43 years. The mean seasonal variation in RT was more than 290%. However, it shows an increasing pattern from the northwestern to southeastern area of the Bohai Sea. In addition, there is evident spatial variation in the maximum and minimum values of RT with respect to the seasons and months. Sensitivity experiments suggest that the monsoon wind is the dominant factor affecting the seasonal variation in the RT within the Bohai Sea. The annual mean RT increased by approximately 90% and the SV decreased significantly over the entire Bohai Sea if the winds were removed from the hydrodynamic model, suggesting that wind could enhance the water exchange and play an important role in the seasonal variation in the RT. Wind could enhance the residual currents in the Bohai Sea and thus accelerate the water exchange rate of the Bohai Sea. The residual currents vary seasonally because of the seasonal shift of the monsoon wind, which induces the seasonal variability of RT in the Bohai Sea. Sensitivity experiments show that the effects of tides, baroclinic processes, and river runoff on seasonal variations in RT within the Bohai Sea are much weaker than those of the wind. The tidal effect on the seasonal variation in RT is mainly located in the BS and BHB, while the effects of river runoff and baroclinic processes are mainly located in the central CB and near the Yellow River estuary.

**Acknowledgments** The authors are grateful to Dr. Haiyan Wang of the National Marine Environmental Forecasting Center, China, for her valuable suggestions.

## References

Bolin B, Rodhe H (1973) A note on the concepts of age distribution and transit time in natural reservoirs. Tellus 25(1):58–62

Bulletin of Chinese river sediment (2015) The Ministry of Water Resources of the People's Republic of China. China Water Power Press, Beijing, Chinese (in Chinese)

Cai Z, Liu Z, Guo X, Gao H, Wang Q (2014) Influences of intratidal variations in density field on the subtidal currents: implication from a synchronized observation by multiships and a diagnostic calculation. J Geophys Res Oceans 119(3):2017–2033

Cheng Y, Mu Z, Wang H, Zhao F, Li Y, Lin L (2019) Water residence time in a typical tributary bay of the three Gorges Reservoir. Water (Switzerland) 11(8):1585

Deleersnijder E, Campin JM, Delhez EJM (2001) The concept of age in marine modelling I. theory and preliminary model results. J Mar Syst 28(3–4):229–267

Delhez EJM (2006) Transient residence and exposure times. Ocean Sci 2(1):1–9

Delhez ÉJM, Deleersnijder É (2002) The concept of age in marine modelling: II. Concentration distribution function in the English Channel and the North Sea. J Mar Syst 31:279–297

Delhez ÉJM, Deleersnijder É (2006) The boundary layer of the residence time field. Ocean Dyn 56(2):139–150

Delhez ÉJM, Heemink AW, Deleersnijder É (2004) Residence time in a semi-enclosed domain from the solution of an adjoint problem. Estuar Coast Shelf Sci 61(4):691–702

Delhez ÉJM, de Brye B, de Brauwere A, Deleersnijder É (2014) Residence time vs influence time. J Mar Syst 132:185–195

Deng Z, Zhao Y (2020) Impact of tidal mixing on water mass properties and circulation in the Bohai Sea: a typhoon case. J Mar Syst 206(January):103338

Ding X, Guo X, Zhang C, Yao X, Liu S, Shi J et al (2020) Water conservancy project on the Yellow River modifies the seasonal variation of chlorophyll-a in the Bohai Sea. Chemosphere 126846

Du J, Shen J (2016) Water residence time in Chesapeake Bay for 1980–2012. J Mar Syst 164:101–111

Du J, Park K, Shen J, Dzwonkowski B, Yu X, Yoon BI (2018) Role of Baroclinic processes on flushing characteristics in a highly stratified estuarine system, Mobile Bay, Alabama. J Geophys Res Oceans 123(7):4518–4537

Duan H, Wang C, Liu Z, Wang H, Wu X, Xu J (2020) Summer wind gusts modulate transport through a narrow strait, Bohai, China. Estuar Coast Shelf Sci 233(September 2019):106526

Ekman VW (1905) On the influence of the Earth's rotation on ocean-currents. Ark Mat Astr Fys 2(11):1–52

Estrade P, Marchesiello P, De Verdière, Colin A, Roy C (2008) Cross-shelf structure of coastal upwelling: a two-dimensional extension of Ekman's theory and a mechanism for inner shelf upwelling shut down. J Mar Res 66(5):589–616

Feng S, Cheng RT, Xi P (1986) On tide-induced Lagrangian residual current and residual transport: a. Lagrangian residual current. Water Resour Res 22(12):1623–1634

Feng S, Ju L, Jiang W (2008) A Lagrangian mean theory on coastal sea circulation with inter-tidal transports I. Fundamentals. Acta Oceanol Sin 27(6):1–16

Gong W, Shen J, Jia J (2008) The impact of human activities on the flushing properties of a semi-enclosed lagoon: Xiaohai, Hainan, China. Mar Environ Res 65(1):62–76

Gourgue O, Deleersnijder E, White L (2007) Toward a generic method for studying water renewal, with application to the epilimnion of Lake Tanganyika. Estuar Coast Shelf Sci 74(4):628–640

Guo X, Hukuda H, Miyazawa Y, Yamagata T (2003) A triply nested ocean model for simulating the Kuroshio—roles of horizontal resolution on JEBAR. J Phys Oceanogr 33(1):146–169

Guo W, Wu G, Xu T, Li X, Ren X, Hao Y (2018) Numerical modelling of temporal and spatial patterns of petroleum hydrocarbons concentration in the Bohai Sea. Mar Pollut Bull 127:251–263

Guyon E, Hulin J-P, Petit L, Mitescu C, Jankowski D (2001) Physical hydrodynamics. Appl Mech Rev 55(5):B96–B97

Huang D, Su J, Backhaus JO (1999) Modelling the seasonal thermal stratification and baroclinic circulation in the Bohai Sea. Cont Shelf Res 19(11):1485–1505

Jenkins WJ (2003) Tracers of ocean mixing. In: Holland HD, K. K. B. T.T. on G. Turekian (eds) Treatise on Geochemistry, pp 223–246

Jiang W, Feng S (2011) Analytical solution for the tidally induced Lagrangian residual current in a narrow bay. Ocean Dyn 61(4): 543–558

Jiang W, Feng S (2014) 3D analytical solution to the tidally induced Lagrangian residual current equations in a narrow bay. Ocean Dyn 64(8):1073–1091

Jordi A, Basterretxea G, Wang DP (2011) Local versus remote wind effects on the coastal circulation of a microtidal bay in the Mediterranean Sea. J Mar Syst 88(2):312–322

Ju X, Ma C, Yao Z, Bao X (2020) Case analysis of water exchange between the Bohai and Yellow Seas in response to high winds in winter. J Oceanol Limnol 38(1):30–41

Li X, Yuan D, & Sun J (2009) Simulation of water exchange in Bohai bay. Advances in Water Resources and Hydraulic Engineering - Proceedings of 16th IAHR-APD Congress and 3rd symposium of IAHR-ISHS, 1341–1346

Li J, Dong H, Zhang D, Han B, Zhu C, Liu S, Liu X, Ma Q, Li X (2015a) Sources and ecological risk assessment of PAHs in surface sediments from Bohai Sea and northern part of the Yellow Sea, China. Mar Pollut Bull 96(1–2):485–490

Li Y, Wolanski E, Zhang H (2015b) What processes control the net currents through shallow straits? A review with application to the Bohai Strait, China. Estuar Coast Shelf Sci 158:1–11

Li Z, Wang H, Guo X, Liu Z, Gao H, Zhang G (2017) Influence of a water regulation event on the age of Yellow River water in the Bohai. J Ocean Univ China 16(5):727–737

Lin L, Liu Z (2019a) Partial residence times: determining residence time composition in different subregions. Ocean Dyn 69(9):1023–1036

Lin L, Liu Z (2019b) TVDal: total variation diminishing scheme with alternating limiters to balance numerical compression and diffusion. Ocean Model 134:42–50

Lin L, Liu Z, Xie L, Gao H, Cai Z, Chen Z, Zhao J (2015) Dynamics governing the response of tidal current along the mouth of Jiaozhou Bay to land reclamation. J Geophys Res Oceans 120(4):2958–2972

Lin L, Liu D, Guo X, Luo C, Cheng Y (2020) Tidal effect on water export rate in the eastern shelf seas of China. J Geophys Res Oceans 125(5)

Liu Z, Wei H, Liu G, Zhang J (2004) Simulation of water exchange in Jiaozhou Bay by average residence time approach. Estuar Coast Shelf Sci 61(1):25–35

Liu Z, Wang H, Guo X, Wang Q, Gao H (2012) The age of Yellow River water in the Bohai Sea. J Geophys Res Oceans 117(11):1–19

Liu Z, Lin L, Xie L, Gao H (2016) Partially implicit finite difference scheme for calculating dynamic pressure in a terrain-following co-ordinate non-hydrostatic ocean model. Ocean Model 106:44–57

Liu J, Du J, Yi L (2017) Ra tracer-based study of submarine groundwater discharge and associated nutrient fluxes into the Bohai Sea, China: a highly human-affected marginal sea. J Geophys Res Oceans 122(11):8646–8660

Liu X, Dunne JP, Stock CA, Harrison MJ, Adcroft A, Resplandy L (2019) Simulating water residence time in the coastal ocean: a global perspective. Geophys Res Lett 46(23):13910–13919

Matsumoto K, Takanezawa T, Ooe M (2000) Ocean tide models developed by assimilating TOPEX/POSEIDON altimeter data into hydrodynamical model: a global model and a regional model around Japan. J Oceanogr 56(5):567–581

Mellor GL (2002) Users guide for a three-dimensional, primitive equation, numerical ocean model. Ocean Model 8544(June):0710

Mitarai S, Siegel DA, Watson JR, Dong C, McWilliams JC (2009) Quantifying connectivity in the coastal ocean with application to the Southern California Bight. J Geophys Res Oceans 114(10):1–21

Monismith S (1986) An experimental study of the upwelling response of stratified reservoirs to surface shear stress. J Fluid Mech 171:407–439

Patankar Suhas V (1980) Numerical heat transfer and fluid flow. New York: McGraw-Hill. p. 102. ISBN 0-89116-522-3

Pfeiffer-Herbert AS, Kincaid CR, Bergondo DL, Pockalny RA (2015) Dynamics of wind-driven estuarine-shelf exchange in the Narragansett Bay estuary. Cont Shelf Res 105:42–59

Safak I, Wiberg PL, Richardson DL, Kurum MO (2015) Controls on residence time and exchange in a system of shallow coastal bays. Cont Shelf Res 97:7–20

Santos IR, Burnett WC, Chanton J, Dimova N, Peterson RN (2009) Land or ocean?: assessing the driving forces of submarine groundwater discharge at a coastal site in the gulf of Mexico. J Geophys Res Oceans 114(4):1–11

Shen J, Gong W (2009) Influence of model domain size, wind directions and Ekman transport on storm surge development inside the Chesapeake Bay: a case study of extratropical cyclone Ernesto, 2006. J Mar Syst 75(1–2):198–215

Shen J, Haas L (2004) Calculating age and residence time in the tidal York River using three-dimensional model experiments. Estuar Coast Shelf Sci 61(3):449–461

Sun J, Lin B, Li K, Jiang G (2014) A modelling study of residence time and exposure time in the Pearl River Estuary, China. J Hydro Environ Res 8(3):281–291

Takeoka H (1984) Fundamental concepts of exchange and transport time scales in a coastal sea. Cont Shelf Res 3(3):311–326

Wan Y, Qiu C, Doering P, Ashton M, Sun D, Coley T (2013) Modeling residence time with a three-dimensional hydrodynamic model: linkage with chlorophyll a in a subtropical estuary. Ecol Model 268:93–102

Wang D-P, Elliott AJ (1978) Non-tidal variability in the Chesapeake Bay and Potomac River: evidence for non-local forcing. J Phys Oceanogr 8(2):225–232

Wang Q, Guo X, Takeoka H (2008) Seasonal variations of the Yellow River plume in the Bohai Sea: a model study. J Geophys Res Oceans 113(8):1–14

Wang H, Gao Z, Zou T, Liu G, Liu Z (2010a) Freshwater residence time in the Bohai Sea. Chin J Ecol 29(3):498–503 (in Chinese with English abstract)

Wang J, Shen Y, Guo Y (2010b) Seasonal circulation and influence factors of the Bohai Sea: a numerical study based on Lagrangian particle tracking method. Ocean Dyn 60(6):1581–1596

Wei H, Wu J-p, Pohlmann T (2001) A simulation on the seasonal variation of the circulation and transport in the Bohai Sea. J Oceanogr Huanghai Bohai Seas 19(02):1–9

Wei H, Hainbucher D, Pohlmann T, Feng S, Suendermann J (2004) Tidal-induced Lagrangian and Eulerian mean circulation in the Bohai Sea. J Mar Syst 44(3–4):141–151

Wu X, Wu H, Wang H, Bi N, Duan H, Wang C, Bian C, Xu J (2019) Novel, repeated surveys reveal new insights on sediment flux through a Narrow Strait, Bohai, China. J Geophys Res Oceans 124(10):6927–6941

Yang S, Lee D, Ho T (2012) The isotopic composition of cadmium in the water column of the South China Sea. Geochim Cosmochim Acta 98:66–77

Yuan D, Lin B, Falconer RA (2007) A modelling study of residence time in a macro-tidal estuary. Estuar Coast Shelf Sci 71(3–4):401–411

Zhang H, Cheng W, Chen Y, Shi Z, Gong W, Liu S (2019) Importance of large-scale coastal circulation on bay-shelf exchange and residence time in a subtropical embayment, the northern South China Sea. Ocean Coast Manag 168:72–89

Zhao J, Ran W, Teng J, Liu Y, Liu H, Yin X et al (2018) Microplastic pollution in sediments from the Bohai Sea and the Yellow Sea, China. Sci Total Environ 640–641:637–645

Zhou F, Huang D, Xue H, Xuan J, Yan T, Ni X, Zeng D, Li J (2017) Circulations associated with cold pools in the Bohai Sea on the Chinese continental shelf. Cont Shelf Res 137:25–38

Zhuang W, Gao X (2015) Distributions, sources and ecological risk assessment of arsenic and mercury in the surface sediments of the southwestern coastal Laizhou Bay, Bohai Sea. Mar Pollut Bull 99(1–2):320–327

Zimmerman JTF (1976) Mixing and flushing of tidal embayments in the western Dutch Wadden Sea part I: distribution of salinity and calculation of mixing time scales. Neth J Sea Res 10(2):149–191

Zimmerman JTF (1979) On the Euler-Lagrange transformation and the stokes' drift in the presence of oscillatory and residual currents. Deep Sea Research Part . Oceanogr Res Papers, 26(5), 505–520